IEEE Sensors Letters Volume X(X) (2018)
Capacitive MEMS Inertial Sensors

Dual-Axis Accelerometer Design and Analysis

Paolo M. Arguelles[1*]

[1] *School of Electrical and Computer Engineering, Cornell University, Ithaca, NY 14850, USA*
[*] *Member, IEEE*

Received 10 Nov 2018.

Abstract—A capacitive sensing scheme to implement a dual-axis MEMS accelerometer using a single proof mass is presented in this paper. The proposed design uses a combination of cantilever and folded beams placed along a single device axis to realize dual-axis motion. COMSOL Multiphysics® modeling software was used to computationally validate theoretical MATLAB analyses by performing eigenfreguency, parametric sweep, and frequency sweep studies on the physical system, taking into account any air-damping effects caused by movement of the proof mass over the underlying substrate. The final design achieves resonant frequencies of 1.5 kHz and 2.3 kHz, and sensitivities of 27.6 mV/(m/s^2) and 11.2 mV/(m/s^2) in the x- and y-axes, respectively, in a footprint less than 2 mm by 2 mm in size. Further simulations and MATLAB analysis find the proposed device to be in compliance with all imposed design requirements and constraints.

Index Terms—MEMS, capacitive sensing, accelerometer, dual-axis

I. INTRODUCTION

Many commercial-off-the-shelf accelerometers such as the ADXL193 and the A600 series only offer single-axis sensing [1], [5]. A trivial way to implement multi-axial sensing is by effectively stacking, or positioning multiple single-axis accelerometers in various axes. However, this would increase the sensor footprint unneededly [4], as well as drive up manufacturing costs; methods to realize multi-axial sensing with a single proof mass are favored [1] - [3]. This paper presents a scheme to implement an accelerometer capable of dual-axis sensing using one proof mass. This paper will discuss the mechanical and electrical principles of operation, design requirements and proposed geometry of the accelerometer, simulation results from COMSOL Multiphysics®, and MATLAB analyses. The proposed device is designed for a dynamic range of ± 5 G, and is realizable in a footprint no larger than 2mm by 2mm. The design consists of two cantilever beams and four folded beams to realize multiaxial motion in a capacitive sensing scheme.

II. MECHANICAL THEORY OF OPERATION

The proposed accelerometer consists of a differential capacitive sensing element, whose capacitance varies according to acceleration [3]. When an external force is applied to the system, the proof mass is perturbed, and a sensing finger attached to the proof mass is displaced from the center of an electrode pair, changing the capacitance between the finger and each electrode. Using a voltage divider configuration, with the impedance of each capacitor acting as the voltage dividers,

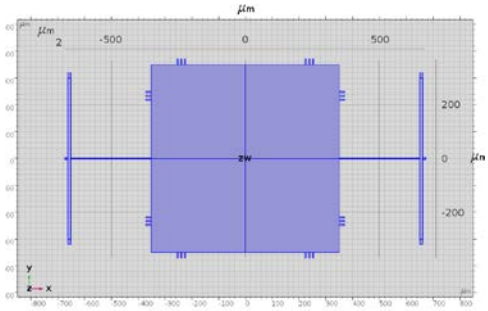

Fig. 1. Geometry of proposed two-axis accelerometer

The proof mass is suspended at the center of the system by cantilever beams, which act as springs in a damped mass system to elicit a predictable displacement given an input force in the axis transverse to the beams. To detect acceleration in the other axis, the cantilever beams are attached to a set of guided beams to enable compliance in both axes. The structural topology of the proof mass and cantilever beams is shown in Fig. 1.

A. Calculation of Resonance Frequencies

The geometry described above suggests an asymmetry between both axes. Naturally, the proof mass will have greater compliance in the y-direction than in the x-direction. The equation for spring constant in the x-direction was calculated to be

$$k_x = 2\left(\frac{E_{\mathrm{Si}} t W_x^3}{L_x^3}\right) \quad (1)$$

where E_{Si} is the Young's modulus of silicon, t is the thickness of the beam, W_i and L_i is the width and length of the beam, respectively, for motion in an i-axis. The spring constant in the x-direction shown above is consistent wit h four folded cantilever beams for comb drives, each with a spring constant of

$$k = \frac{E_{\mathrm{Si}} t W_x^3}{2L_x^3}, \quad (2)$$

Corresponding author: P. M. Arguelles (pa394@cornell.edu).
Digital Object Identifier: 10.1109/LSEN.XXXX.XXXXXXX (inserted by IEEE).

in parallel. The equation for spring constant in the y-direction was calculated to be

$$k_y = \frac{1}{2}\left(\frac{EtW_y^3}{L_y^3}\right).$$

Because the end of each cantilever beam allowing motion in the y-direction is not anchored, and instead attached to another set of springs, each beam may be modeled as a free cantilever beam, each with a spring constant of

$$k = \frac{E_{\mathrm{Si}} t W_x^3}{4L_x^3}. \quad (4)$$

The y-direction spring constant shown above is consistent with two free cantilever beams in parallel. The proof mass *m* was calculated by multiplying each proof mass dimension by the density of silicon ρ_{Si}.

$$m = \rho_{\mathrm{Si}} t_{\mathrm{mass}} w_{\mathrm{mass}} h_{\mathrm{mass}} \quad (5)$$

The resonance frequency for motion in the i-axis was calculated by:

$$\omega_i = \sqrt{\frac{k_i}{m}} \quad (6)$$

B. Damping Calculations

The damping coefficient *b* is expressed by:

$$b = \frac{A\mu}{h} \quad (7)$$

where *A* is the area of overlap between the proof mass and underlying substrate (this is equivalent to the area of the proof mass), *h* is the gap between the proof mass and substrate, and μ is the viscosity of air. Here, $\mu = 1.83 \times 10^{-5}$ kg/(m · s), which is the dynamic viscosity of air at room temperature. The quality factor *Q* may in turn be derived from *b* by:

$$Q = \frac{\sqrt{km}}{b} \quad (8)$$

III. ELECTRICAL THEORY OF OPERATION

A. Sensitivity of a Capacitive Sensor

Consider a simplified version of the sensing circuit comprised of one pair of differential capacitors. The voltage on the sensing finger may be determined by voltage division:

$$V = \frac{Z_{C1}}{Z_{C1} + Z_{C2}} V_{DD} = \frac{1}{1 + \frac{d_0 - x}{d_0 + x}} V_{DD} \quad (9)$$

From this equation, an expression for *x* in terms of *V* can be determined:

$$x = d_0 - \frac{2d_0}{V_{DD}} V \quad (10)$$

Combining Hooke's Law ($F = kx$) and Newton's Second Law ($F = ma$):

$$x = \frac{m}{k} a. \quad (11)$$

This may be substituted in the equation found for the differential capacitors,

$$\frac{m}{k} a = d_0 - \frac{2d_0}{V_{DD}} V. \quad (12)$$

Solving this equation for *V* to get a mathematical relationship between *V* and *a*:

$$V(a) = -\frac{mV_{DD}}{2d_0 k} a + \frac{V_{DD}}{2}. \quad (13)$$

The sensitivity of a sensor is defined as the change in the output quantity over the change in the input (or sensed) quantity. In this case, the output quantity is voltage *V*, and the sensed quantity is acceleration *a*: (3)

$$\text{sensitivity} = \left|\frac{dV}{da}\right| \quad (14)$$

Taking the derivative of *V(a)* yields an equation for sensitivity:

$$\text{sensitivity} = \left|\frac{dV}{da}\right| = \frac{mV_{DD}}{2d_0 k} \quad (15)$$

IV. DESIGN REQUIREMENTS AND ANALYSIS

The accelerometer should comply with all design requirements tabulated below.

Table 1. Requirements

No.	Parameter	Specification
1.1	V_{DD}	5 V
1.2	Resonant frequency in X	< 2.5 kHz
1.3	Resonant frequency in Y	< 2.5 kHz
1.4	Sensitivity in X	> 10 mV/(m/s^2)
1.5	Sensitivity in Y	> 10 mV/(m/s^2)
1.6	Non-linearity in 100 Hz – 500 Hz	Minimize
1.7	Dynamic Range	± 5 G
1.8	Design Area	Minimize (2 mm x 2 mm)
1.9	Material	Single-crystal silicon (5 µm thick)
1.10	Minimum lithography feature	1 um
1.11	Spacing to substrate	5 um

The requirements were found to be satisfied by the design parameters listed below.

Table 2. Design Parameters

Parameter	Value
Extruding length	5 µm
Proof mass width	700 µm
Proof mass length	700 µm
Sensing finger length	0.02 mm
Sensing finger width	5 µm
Gap between sensing finger and electrode	1 µm
Beam width	2 µm
Beam length	300 µm

The proof mass and cantilever design parameters in Table 2 were selected such that the resonance frequencies in the x- and y-axes would be lower than 2.5 kHz, and therefore comply with Requirements 1.2 and 1.3 (Table 1). The final resonances were found to be $\omega_x = 1.5$ kHz and $\omega_y = 2.3$ kHz.

V. COMSOL SIMULATION RESULTS

COMSOL Multiphysics® modeling software was used to With the exception of the *Eigenfrequency Study*, all simulations were performed taking into account the damping effects of the proof mass moving over the substrate in air.

A. Eigenfrequency Study

The *Eigenfrequency Study* was used to analytically determine the bending modes of the system, as well as their corresponding eigenfrequencies. Figs. 2 and 3 depict the bending modes of the damped mass system in the x- and y-axes, respectively. The color map corresponds to change in displacement given the calculated eigenfrequency.

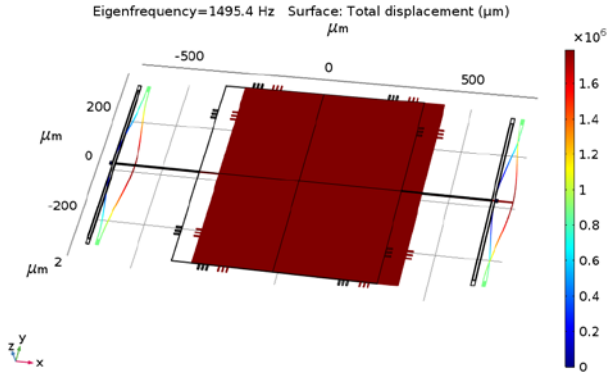

Fig. 2. The bending mode depicting movement in the x-direction, and its associated eigenfrequency.

The resonance frequency of the x-axis bending mode (Fig. 2), was found to be 1.5 kHz.

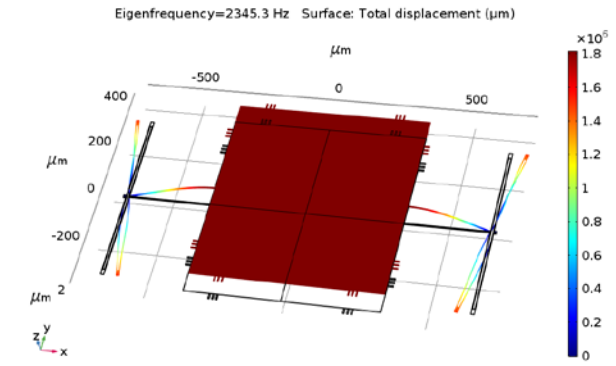

Fig. 3. The bending mode depicting movement in the y-direction, and its associated eigenfrequency.

The resonance frequency of the y-axis bending mode (Fig. 3), was found to be 2.3 kHz.

B. Sensitivity Analysis

A sensitivity analysis was performed in both axes by varying the magnitude of the boundary load exerted on the proof mass, and determining the corresponding response of the sensor in the form of displacement. Plotting the resulting data, the sensitivity of the sensor may be estimated by the slope of the line of best fit. This study was conducted in COMSOL by applying a *Parametric Sweep* to a *Stationary Study*. The simulation was programmed to iterate through a range of forces corresponding to ± 10 G. The resulting x- and y-axis plots are shown in Figs. 4 and 5, respectively.

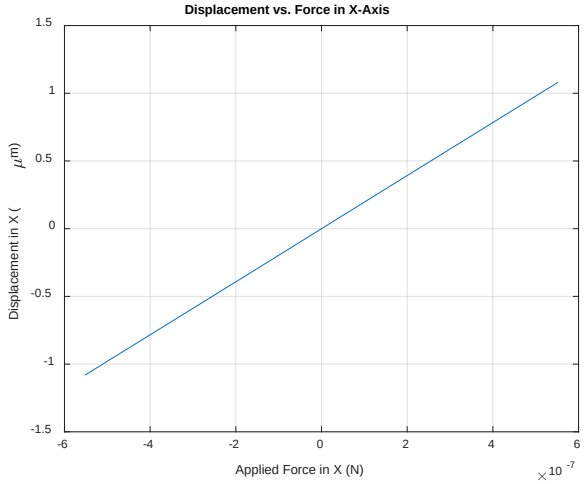

Fig. 4. Displacement as a function of applied force in the x-direction. Forces were varied in a parametric sweep from -10 G to 10 G.

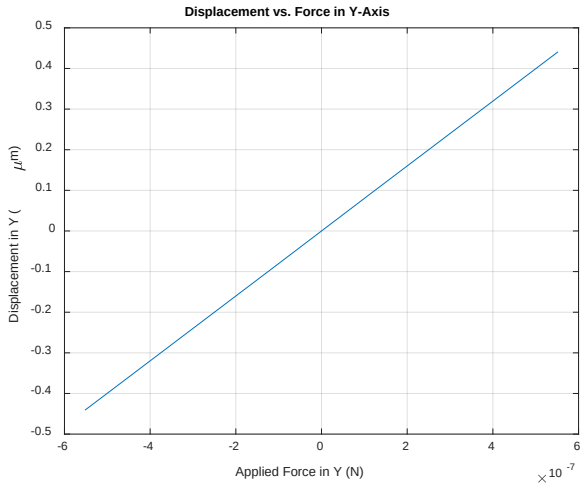

Fig. 5. Displacement as a function of applied force in the y-direction. Forces were varied in a parametric sweep from -10 G to 10 G.

The structural analysis performed in COMSOL Multiphysics yields sensitivity data in displacement per unit force, or meters per Newton.

$$\text{slope} = \frac{x}{F} = \frac{x}{ma} \tag{16}$$

Combining Eq. (6) with Eq. (10):

$$\text{slope} = \frac{x}{F} = \frac{d_0 - \frac{2d_0}{V_{DD}}V}{ma} \tag{17}$$

Sensitivity in units of voltage per unit acceleration is given by:

$$\frac{V}{a} = \text{slope} \cdot \left(\frac{mV_{DD}}{2d_0}\right) \tag{18}$$

The slopes of the sensitivity lines in Figs. 4 and 5 are 0.80 m/N for motion in the y-axis, and 1.96 m/N for motion in the x-axis. Calculating sensitivity in terms of volts per acceleration using Eq.

(18) yields 11.2 $\frac{\text{mV}}{\text{m/s}^2}$ for the y-axis, and 14.1 $\frac{\text{mV}}{\text{m/s}^2}$ for the x-axis. These results comply with the sensitivity requirements 1.4 and 1.5 in Table 1.

C. Dynamic Range Test

Requirement 1.7 (Table 1) dictates that dynamic range of the accelerometer correspond to ± 5 G. Figs. 4 and 5 correspond to this dynamic range, and show ideal linearity throughout the range. The dynamic range is limited by the physical structure of the sensor, specifically the spacer parameter value. In the proposed design, the spacer has a value of 1 µm, the smallest allowable dimension. A DC input force in the x-direction of 5 G representing the upper limit of the desired dynamic range, for instance, would yield a displacement of just over 0.5 µm (Fig. 4). Because the spacer is 1 µm in length, a 0.5 µm displacement is easily achievable. A DC input force of 5 G in the y-direction yields a displacement of about 0.23 µm. However, since motion in the y-axis is not functionally limited by the structure, the sensor is able to realize unobstructed, linear motion in this axis as well.

D. Linearity Study

Linearity is vital to maintaining the integrity of a sensor reading. Ideally, the accelerometer should be designed such that the system is robust against inputs with varying frequency. For instance, in this accelerometer, the displacement peaks at resonance. In this scenario, the voltage seen across the capacitor divider would correspond to a force much larger than what was actually applied, and affect the integrity of the reading. Requirement 1.6 (Table 1) ensures that the response of this accelerometer is linear, or its linearity minimized, for low-frequency inputs. The linearity study was conducted for both axes in COMSOL Multiphysics by setting the boundary load of the relevant axis equal to the force generated on the proof mass by 1 G of acceleration, and performing a frequency sweep from 100 Hz to 500 Hz, with discrete steps of 100 Hz. Performing the frequency domain analysis yielded complex displacement values; only the real components were plotted.

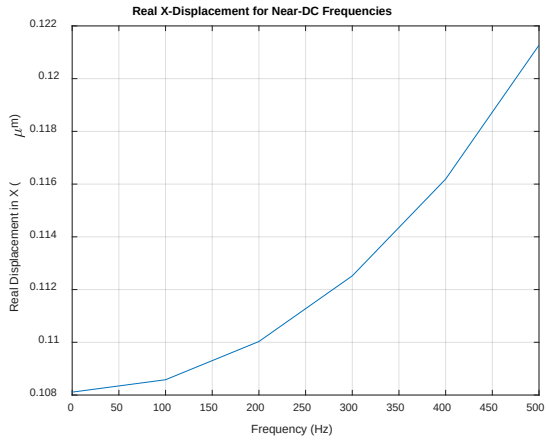

Fig. 6. Linearity test in x-axis for near-DC frequencies. Frequency was swept from 100 Hz to 500 Hz in increments of 100 Hz.

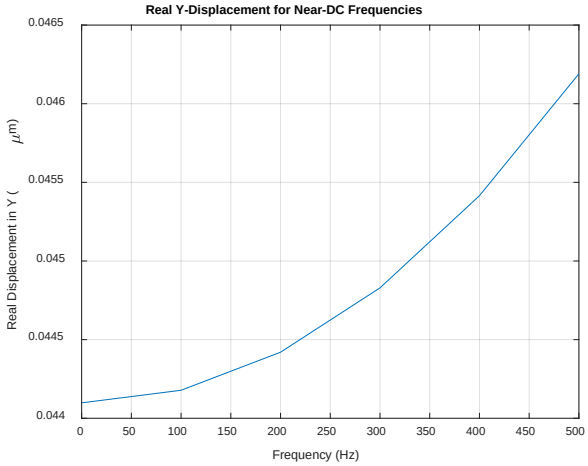

Fig. 7. Linearity test in y-axis for near-DC frequencies. Frequency was swept from 100 Hz to 500 Hz in increments of 100 Hz.

To determine the displacement of the proof mass at low, high, and resonance frequencies, begin with a motion equation. The motion of an oscillatory damped mass system, which the accelerometer presented here is an example, may be characterized by the following differential equation:

$$m\frac{d^2x}{dt^2} + b\frac{dx}{dt} + kx = F \tag{19}$$

Applying the Fourier transform and solving for *x*, an equation relating displacement and frequency may be established:

$$X(\omega) = \frac{\frac{F}{m}}{\omega_0^2 - \omega^2 + j\frac{\omega\omega_0}{Q}} \tag{20}$$

Taking the absolute value and plotting the output with respect to frequency yields the magnitude plots shown in Figs. 8 and 9.

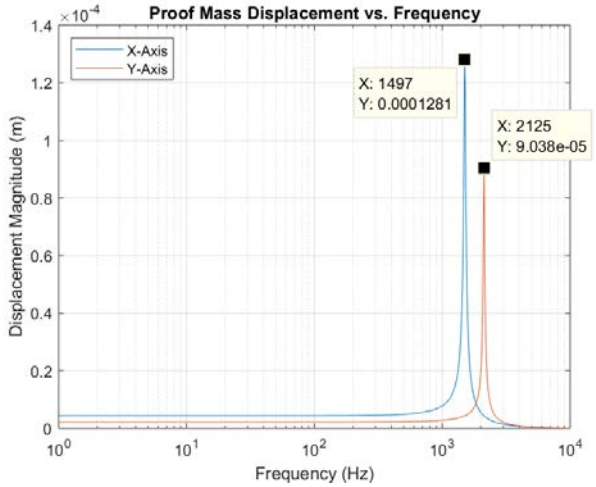

Fig. 8. Proof mass displacement as a function of frequency, expressed in meters. Frequency sweep analysis was performed for a boundary load equivalent to 1 G acting on the proof mass.

Examining Fig. 8, the displacement due to a 1 G acceleration at very low frequencies is 4.4 µm for a force exerted in the x-axis, and 2.2 µm for the y-axis. At resonance, the displacement peaks at

128 μm for the x-axis, and 90.4 μm for the y-axis. At very high frequencies, the displacements in both axes tend toward zero.

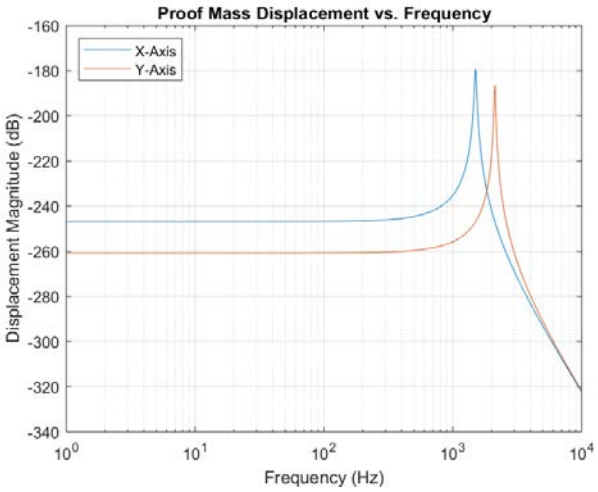

Fig. 9. Proof mass displacement as a function of frequency, expressed in decibels. Frequency sweep analysis was performed for a boundary load equivalent to 1 G acting on the proof mass.

A summary of these findings above is tabulated below (Table 3).

Table 3. Displacement at Varying Frequencies

Frequency	Displacement
0	4.4 μm (x-axis) 2.2 μm (y-axis)
ω_0	128.1 μm (x-axis) 90.4 μm (y-axis)
∞	0 μm

VI. CONCLUSION

This paper presents a topology to implement dual-axis sensing for a MEMS accelerometer using a single proof mass. The final design has been shown to meet and/or exceed all listed design requirements and constraints (Table 5).

Table 5. Requirement Compliance

No.	Specification	Actual
1.1	5 V	5 V
1.2	**< 2.5 kHz**	**1.5 kHz**
1.3	**< 2.5 kHz**	**2.3 kHz**
1.4	**> 10 mV/(m/s^2)**	**27.6 mV/(m/s^2)**
1.5	**> 10 mV/(m/s^2)**	**11.2 mV/(m/s^2)**
1.6	**Minimize**	**Minimize**
1.7	± 5 G	± 5 G
1.8	**2 mm x 2 mm**	**1.36 mm x 0.80 mm**
1.9	**Single-crystal silicon (5 μm thick)**	**Single-crystal silicon (5 μm thick)**
1.10	1 um	1 um
1.11	5 um	5 um

Furthermore, MATLAB and COMSOL Multiphysics analyses proved complementary, offering corroborating accounts as to the compliance of the system to the requirements listed in Table 1.

Table 4. MATLAB vs. COMSOL Multiphysics Results

Parameter	MATLAB (Theoretical)	COMSOL (Analytical)
Spring constant (x-axis)	0.5007 N/m	0.5102 N/m
Spring constant (y-axis)	1.0015 N/m	1.2523 N/m
Resonance frequency (x-axis)	1.50 kHz	1.4954 kHz
Resonance frequency (y-axis)	2.12 kHz	2.35 kHz
Sensitivity (x-axis)	28.1 mV/(m/s^2)	27.6 mV/(m/s^2)
Sensitivity (y-axis)	14.1 mV/(m/s^2)	11.2 mV/(m/s^2)

Comparing the MATLAB and COMSOL Multiphysics columns, the calculated sensitivity drops. This makes intuitive sense, as the COMSOL Multiphysics simulation takes into account the damping effects of the proof mass movement over the underlying substrate on what is essentially an air cushion. The spring constants are also slightly higher in the latter case, as the MATLAB scripts simplistically approximate the spring system as a combination of either free or guided cantilever beams. Overall, the theoretical values and analytically derived counterparts seem to agree within a reasonable margin, offering an experimental validation of the operating principles behind a capacitive, dual-axis, MEMS accelerometer.

REFERENCES

[1] A. Aydemir and T. Akin, "Fabrication of a three-axis capacitive MEMS accelerometer on a single substrate," *2015 IEEE Sensors*, 2015.

[2] D. Chattaraj, K. B. M. Swamy, and S. Sen, "Design and analysis of dual axis MEMS accelerometer," *2007 International Workshop on Physics of Semiconductor Devices*, 2007.

[3] J. Nazdrowicz, "SIMULINK and COMSOL software application for MEMS accelerometer modeling and simulation," *2017 MIXDES - 24th International Conference "Mixed Design of Integrated Circuits and Systems*, 2017.

[4] T. Sethuramalingam and A. Vimalajuliet, "Design of MEMS based capacitive accelerometer," *2010 International Conference on Mechanical and Electrical Technology*, 2010.

[5] S. Sherman, H. Samuels, and W. Riedel, "A Low Cost Dual Axis Accelerometer," *SAE Technical Paper Series*, 1997.